J Comput Aided Mol Des (2011) 25:413–426
DOI 10.1007/s10822-011-9428-y

Molecular dynamics simulations of pro-apoptotic BH3 peptide helices in aqueous medium: relationship between helix stability and their binding affinities to the anti-apoptotic protein Bcl-X_L

Dilraj Lama · Ramasubbu Sankararamakrishnan

Received: 9 December 2010 / Accepted: 11 April 2011 / Published online: 27 April 2011

Abstract The B-cell lymphoma 2 (Bcl-2) family of proteins regulates the intrinsic pathway of apoptosis. Interactions between specific anti- and pro-apoptotic Bcl-2 proteins determine the fate of a cell. Anti-apoptotic Bcl-2 proteins have been shown to be over-expressed in certain cancers and they are attractive targets for developing anti-cancer drugs. Peptides from the BH3 region of pro-apoptotic proteins have been shown to interact with anti-apoptotic Bcl-2 proteins and induce biological activity similar to that observed in parent proteins. However, the specificity of BH3 peptides derived from different pro-apoptotic proteins differ for different anti-apoptotic Bcl-2 proteins. In this study, we have investigated the relationship between the stable helical nature of BH3 peptides and their affinities to Bcl-X_L, an anti-apoptotic Bcl-2 protein. We have carried out molecular dynamics simulations of six BH3 peptides derived from Bak, Bad and Bim pro-apoptotic proteins for a period of 50 ns each in aqueous medium. Due to the amphipathic nature of BH3 peptides, the hydrophobic residues on the hydrophobic face tend to cluster together in all BH3 peptides. While this process resulted in a complete loss of helical structure in 16-mer Bak and 16-mer Bad wild type peptides, stabilizing interactions in the hydrophilic face of the BH3 peptides and capping interactions helped to maintain partial helical character in 16-mer Bad mutant and 16-mer Bim peptides. The latter two 16-mer peptides exhibit higher affinity for Bcl-X_L. Similarly the longer BH3 peptides, 25-mer Bad and 33-mer Bim, also resulted in smaller and stable helical fragments and their helical conformation is stabilized by interactions between residues in the solvent-exposed hydrophilic half of the peptide. The stable nature of helical segment in a BH3 peptide can be directly correlated to its binding affinity and the helical region encompassed the highly conserved Leu residue. We propose that upon approaching the hydrophobic groove of anti-apoptotic proteins, a longer helix will be induced in high affinity BH3 peptides by extending the smaller stable helical segments around the conserved Leu residue in both N- and C-terminal regions. The results reported in this study will have implications in developing peptide-based inhibitors for anti-apoptotic Bcl-2 proteins.

Keywords Helix stability · Peptide conformation · Anti-cancer drugs · Peptoid inhibitors · Conformational smapling · Hydrophobic clustering · Capping interactions · Amphipathic helix

Introduction

Structure-based drug design requires knowledge of three-dimensional structures of protein targets and the nature of binding sites of ligand molecules. This approach has successfully identified compounds that have been introduced into clinical trials and eventually approved as drugs [1]. Although potential ligands are small organic molecules for many biomolecular targets, small peptides or peptide-based ligands have been identified as potential inhibitors in targets like Bcl-2 family of proteins [2] or G-Protein Coupled Receptors [3]. Small peptides are usually very flexible in aqueous solution and conformationally stable secondary structures are often induced by the environment [4] or due

Electronic supplementary material The online version of this article (doi:10.1007/s10822-011-9428-y) contains supplementary material, which is available to authorized users.

D. Lama · R. Sankararamakrishnan (✉)
Department of Biological Sciences and Bioengineering, Indian Institute of Technology Kanpur, Kanpur 208016, India
e-mail: rsankar@iitk.ac.in

to the secondary structure propensity of the amino acids of the peptide [5]. Conformational sampling of such peptide ligands is one way to find out their preferred secondary structures in aqueous medium. Both the plasticity of target binding site and the preferred conformations of ligands together play a significant role in determining the affinity of the ligands for the targets. We have recently carried out molecular dynamics simulations of anti-apoptotic Bcl-X_L structures in complex with three peptide ligands from the pro-apoptotic proteins [6]. Bcl-X_L belongs to the Bcl-2 (B cell leukemia/lymphoma 2) family of proteins and members of this family play a critical role in the regulation of the intrinsic pathway of apoptosis [7–9]. Bcl-2 family comprises of both anti- and pro-apoptotic proteins [10]. Protein–protein interaction between the functionally opposing members of the same Bcl-2 family is a crucial event and is one of the ways apoptosis is regulated [7]. Experimental studies have shown that peptides derived from the BH3 domain of pro-apoptotic Bcl-2 proteins are sufficient to interact with anti-apoptotic proteins and also induce cell death [11–16]. Structures of Bcl-2 anti-apoptotic proteins in complex with BH3 peptides from their pro-apoptotic counterparts reveal that the BH3 peptides adopt a well-defined helical structure and dock into the hydrophobic groove present on the surface of the anti-apoptotic protein [17]. However for a specific anti-apoptotic protein, despite apparently similar mode of docking and interactions, different BH3 peptides exhibit wide range of affinities [18, 19]. Simple characterization of experimentally determined complex structures does not explain the differential binding affinities at molecular level. Since Bcl-2 proteins are currently an important target for anti-cancer therapeutics [20, 21] understanding the molecular mechanism of Bcl-2 protein—BH3 peptide binding affinity would help to understand the biology of the Bcl-2 family's role in apoptosis regulation and also significantly aid in the designing of high-affinity inhibitors against specific Bcl-2 proteins.

At least two factors can contribute to higher affinity of a peptide ligand for a particular protein. Specific interactions can occur between particular residues of a peptide ligand and its protein target and such interactions could be clearly an important factor that can give rise to greater affinity compared to other similar peptides lacking those residues. Our previous molecular dynamics (MD) simulations of Bcl-X_L protein in complex with three pro-apoptotic BH3 peptides [6] identified one such arginine residue in the higher affinity BH3 peptide ligands. This Arg could participate in additional stable hydrophobic and hydrophilic interactions with the Bcl-X_L protein. The second important factor is related to the stable nature of a peptide ligand's conformation. This was corroborated by the work of Petros and co-workers [22]. They have earlier investigated BH3 peptide's ability to adopt helical secondary structure in solution and its important influence in the binding affinity to Bcl-X_L [22]. Structures of Bak and Bad BH3 peptides were investigated using CD spectroscopy and there seems to be a direct correlation between the helix-forming tendency of the BH3 peptides and their affinity for Bcl-X_L. The BH3 domain peptides from pro-apoptotic proteins are however reported to be mostly unstructured in aqueous solution [18, 19, 23] whereas in experimentally determined complex structures, they adopt a well-defined helical conformation [11, 17, 22, 24].

It must, however, be pointed out that relatively short and transient helical segments of small peptides will be difficult to identify in CD studies and thus detecting short helical segments in small peptides will be a difficult task in conventional CD spectroscopy. The solution conformation of BH3 peptides in CD studies by Petros et al. [22] provided information on the average helical property and such studies are mostly insensitive to the presence of short helical segments in peptides [25]. However such short helical segments, in contrast to a completely random conformation, could act as nucleation signals for eventually forming a stable helical structure. Molecular dynamics simulations provide an alternative approach to study the ability of a peptide to form stable helical structure and the advantage of this technique is that the details leading to helix folding/unwinding events of a peptide can be studied sequentially at atomic level. Previous simulation studies to investigate the secondary structure of a peptide have been carried out on alanine-based peptides [26, 27], a prion peptide [28], amyloid β-peptide [29] and stapled p53 peptide analogs [30] in explicit solvent. Recently, a molecular dynamics simulation study on the solution conformation of 16-mer peptide belonging to the BH3 region of pro-apoptotic Bak protein showed the presence of substantially stable short helices [31]. This observation was implicated to be important for their binding to Bcl-X_L.

Petros et al. [22] have investigated the secondary structures of Bak and Bad BH3 peptides of different lengths and a possible relationship with their binding affinities to Bcl-X_L. While Bad 16-mer has negligible binding affinity ($K_d > 50{,}000$ nM), the corresponding 16-mer Bak peptide from the same BH3 region shows a remarkably improved binding affinity ($K_d = 480$ nM). The longer Bad 25-mer peptide has the maximum affinity ($K_d = 0.6$ nM) among all wild-type peptides studied. CD studies show that the Bad (16-mer), Bak (16-mer) and Bad (25-mer) peptides have respectively 7, 22 and 44% helical content in 30% TFE solution indicating that the binding affinities and their tendency to form helical secondary structure are correlated. However, the CD studies do not clearly explain the factors that are responsible for giving rise to higher helical content and moreover, what actually stabilizes the helical segments in these small peptides is not

obvious. In this paper, we have carried out molecular dynamics simulations of four Bak and Bad peptides investigated by Petros et al. [22]. Additionally, we have also studied the stability of helical structures of two Bim peptides for comparison purpose and the structure of one of which in complex with the Bcl-X_L protein is available [24]. Our studies clearly indicate that peptides with higher binding affinities have stable helical structures in aqueous medium although the lengths of these helical segments vary. Our analysis explains how these small helical fragments are stabilized when they are present in isolation surrounded by water molecules. Results of this study have implications in designing peptide-based ligands for anti-apoptotic proteins such as Bcl-X_L.

Methods

Description of the starting structures

The starting coordinates for 16-mer Bak, 25-mer Bad and 33-mer Bim BH3 peptides were obtained respectively from Bcl-X_L—Bak (PDB ID: 1BXL [11]), Bcl-X_L—Bad (PDB ID: 1G5 J [22]) and Bcl-X_L—Bim (PDB ID: 1PQ1 [24]) complex structures. Petros et al. [22] generated two 16-mer Bad mutants where some of the residues from the wild type peptide were mutated with the objective to increase the helical character of the 16-mer Bad and correspondingly its affinity for the Bcl-X_L protein. In this study, we considered the mutant with highest helix-forming capability according to the CD studies. Furthermore, we also considered the 16-mer Bim peptide corresponding to the same BH3 region. The starting coordinates for these three additional peptides (16-mer wild type Bad, 16-mer mutant Bad and 16-mer Bim) were obtained from the 25-mer Bad and 33-mer Bim peptides respectively by in silico deletion and mutation of the residues using the Biopolymer module of Insight II (Accelrys, San Diego, CA). The details of the sequences of the selected peptides are shown in Table 1. Residue numbers of the peptides are according to the UniProt [32] accession numbers Q16611, Q61337 and O54918-2 for Bak, Bad and Bim proteins respectively and they correspond to 72–87 for 16-mer Bak, 140–164 for 25-mer Bad and 83–115 for 33-mer Bim.

A total of six different simulations were carried out whose details are mentioned in Table 1. Molecular dynamics simulations were performed using the GROMACS (Ver. 3.2.1) modeling software [33, 34] and the GROMOS96 43a1 force-field [35, 36]. The hydrogen atoms, if present in the experimentally determined structures, were ignored. Using "Pdb2gmx" tool available in GROMACS, hydrogen atoms were added only to polar atoms (nitrogen and oxygen) and aromatic carbon atoms. The N- and C-termini regions of each peptide were capped with NH2 and COOH groups respectively. Default protonation states were assumed for all the titratable residues. The initial peptide structures were first placed in the center of a cubic box. The size of the cubic box was chosen such that the minimum distance between the solute molecule and the edge of the box was at least 15 Å. The solute molecules were then solvated with SPC [37] water molecules using the GROMACS utility program "Genbox". The total number of atoms considered for the six simulations varied between ~21,000 and ~47,000.

Simulation protocol and parameters

The solvated starting structures of the different peptides were initially energy minimized using steepest descent and conjugate gradient methods with harmonic positional restraints applied on the heavy atoms of the solute. The systems were then equilibrated for a period of 2 ns in two stages. First, a 1 ns simulation was performed under NVT (number of atoms, volume and temperature are kept constant) ensemble keeping the harmonic positional restraints on heavy atoms of the solute. The second stage of equilibration consisted of a further 1 ns simulation without any restraints using NPT (constant number of atoms, pressure and temperature) ensemble. A force constant equivalent to 50 kcal/mol-Å^2 was applied on atoms subjected to positional restraints during minimization and equilibration. Production runs constituted 50 ns of MD simulations for each system under NPT condition. SETTLE algorithm was used to constrain the bonds of the solvent molecules [38]. The algorithm LINCS [39] was used to constrain all the bonds involving the hydrogen atoms. Periodic boundary conditions were applied in all the three directions. The simulation temperature and pressure were 300 K and 1 Bar respectively for all the simulations. Temperature was maintained using Berendsen's algorithm [40] with a coupling constant of 0.01 ps during equilibration and 0.05 ps during the production stage. Temperature of the solute and solvent molecules were coupled separately. For pressure coupling, Berendsen's method [40] with a coupling constant of 1.0 ps was used to maintain the boundary pressure. Non-bonded interactions were evaluated using a twin range spherical cutoff of 10 and 18 Å. Leap-frog integrator was used to integrate the equations of motion. A time step of 0.002 ps was used and the non-bonded list for the calculation of van der Waals and electrostatic interactions were updated every 10 steps.

Hydrophobic residue analysis

For each MD simulated peptide structure, distances between center of mass of all possible pairs of hydrophobic

Table 1 Details of the solvated BH3 peptide starting structures used for MD simulations

BH3 peptide	Description of the peptide	Sequence[a]	Length	Total number of atoms
Bak	16-mer Bak	72-GQVGRQ**L**AIIGDDINR-87	16	26741
Bad	25-mer Bad	140-NLWAAQRYGRE**L**RRMSDEFVDSFKK-164	25	21293
	16-mer Bad wt	145-QRYGRE**L**RRMSDEFVD-160	16	22758
	16-mer Bad mutant	145-**DD**Y**A**RE**L**R**MM**A**D**EFV**R**-160[b]	16	21171
Bim	33-mer Bim	83-DLRPEIRIAQE**L**RRIGDEFNETYTRRVFANDYR-115	33	47278
	16-mer Bim	88-IRIAQE**L**RRIGDEFNE-103	16	22653

The 16-mer Bak, 25-mer Bad and 33-mer Bim peptides were obtained from the complex state structure of Bcl-X_L with Bak (PDB ID: 1BXL), Bad (PDB ID: 1G5 J) and Bim (PDB ID: 1PQ1) respectively

[a] The beginning and end residue numbers are given for each peptide sequence which corresponds to their parent protein sequence with Swissprot accession numbers Q16611 (human) for Bak, Q61337 (human) for Bad and O54918-2 (mouse) for Bim. The residue numbering followed for the 16-mer Bad mutant is identical to the 16-mer wild type peptide. The alignment of the peptide sequences is done with reference to the conserved leucine of the BH3 domain (L78 in Bak, L151 in Bad and L94 in Bim) shown in bold, enlarged and underlined

[b] The mutated residues in the mutant are shown in bold with grey background

residues were calculated and the sum of the distances, d_H, is given below in Eq. (1).

$$d_H = \sum d_{ij} \quad (1)$$

where d_{ij} is the center of mass distance between two hydrophobic residues i and j and the sum is over all possible pairs of hydrophobic residues. Analysis of trajectories calculated for d_H will help to understand the overall behavior of hydrophobic residues in a given peptide when they are exposed to aqueous medium.

Results

Secondary structure evolution

A total of six independent simulations were carried out for a period of 50 ns production run each following a 2 ns equilibration of the system. The system properties were analyzed for the entire 52 ns simulation period. The evolution of each peptide's secondary structures was analyzed using the DSSP (Definition of Secondary Structure Prediction) algorithm from Kabsch and Sander [41] (Fig. 1).

The starting structure of the 16-mer Bak peptide is helical from residues 76–84 (Fig. 1a). During the initial stage of the simulation, the peptide shows presence of two helical segments from residues 75–81 and a shorter segment at the C-terminal region from residues 83–86. A similar behavior was observed in an independent simulation of the 16-mer Bak peptide by Yang et al. [31] in which the peptide was simulated for 2 ns using conventional MD followed by 8 ns simulation using self-guided molecular dynamics (SGMD) technique developed by Wu and Wang [42]. It must be pointed out that SGMD can achieve a better conformational sampling compared to conventional MD. Even in this study, DSSP plot shows that only a single helical turn consisting of four residues (residues 76–79) still retained helical conformation at the end of 8 ns of SGMD. In the present longer simulation, we observe that the Bak peptide is no longer helical beyond 25 ns and the peptide structure is predominantly in the random conformation till the end of the simulation period.

The 25-mer Bad peptide is helical from residues 142–158 in the starting structure (Fig. 1b). The peptide looses its helical character in the N-terminal region from 142 to 146 but a stable helical character is maintained between residues 147–158 throughout the simulation. In contrast to the 25-mer peptide, the shorter 16-mer Bad (Fig. 1c) exhibits a random conformation for almost the whole of the simulation period. In fact the DSSP plot shows that it has lost majority of its helical character by the end of 2 ns equilibration and only a short helical segment remained at the C-terminal region when the production run started. The secondary structure of the peptide was further analyzed in detail during the last 1 ns of equilibration period in which no constrains were applied on the system (Fig. 1d). A closer look during this equilibration period indicates that the unwinding of the helix is initiated in the middle region around residues 150–155. This then propagates further towards N-terminus and at the beginning of production run, only a short C-terminal segment still

Fig. 1 Secondary structure evolution of BH3 peptides as evaluated ▶ by DSSP during the entire course of 52 ns MD simulation of which the first 2 ns is the equilibration period. **a** 16-mer Bak, **b** 25-mer Bad, **c** and **d** 16-mer Bad wt, **e** 16-mer Bad mutant, **f** 33-mer Bim and **g** 16-mer Bim. For **d**, the DSSP plot is shown only for the 1 ns restraint free equilibration. The *color codes* for the different structures are *red* β-strand; *blue* α-helix; *green* bend; *yellow* turn; *black* β-bridge; *purple* π-helix; *grey* 3_{10}-helix; *white* coil structure

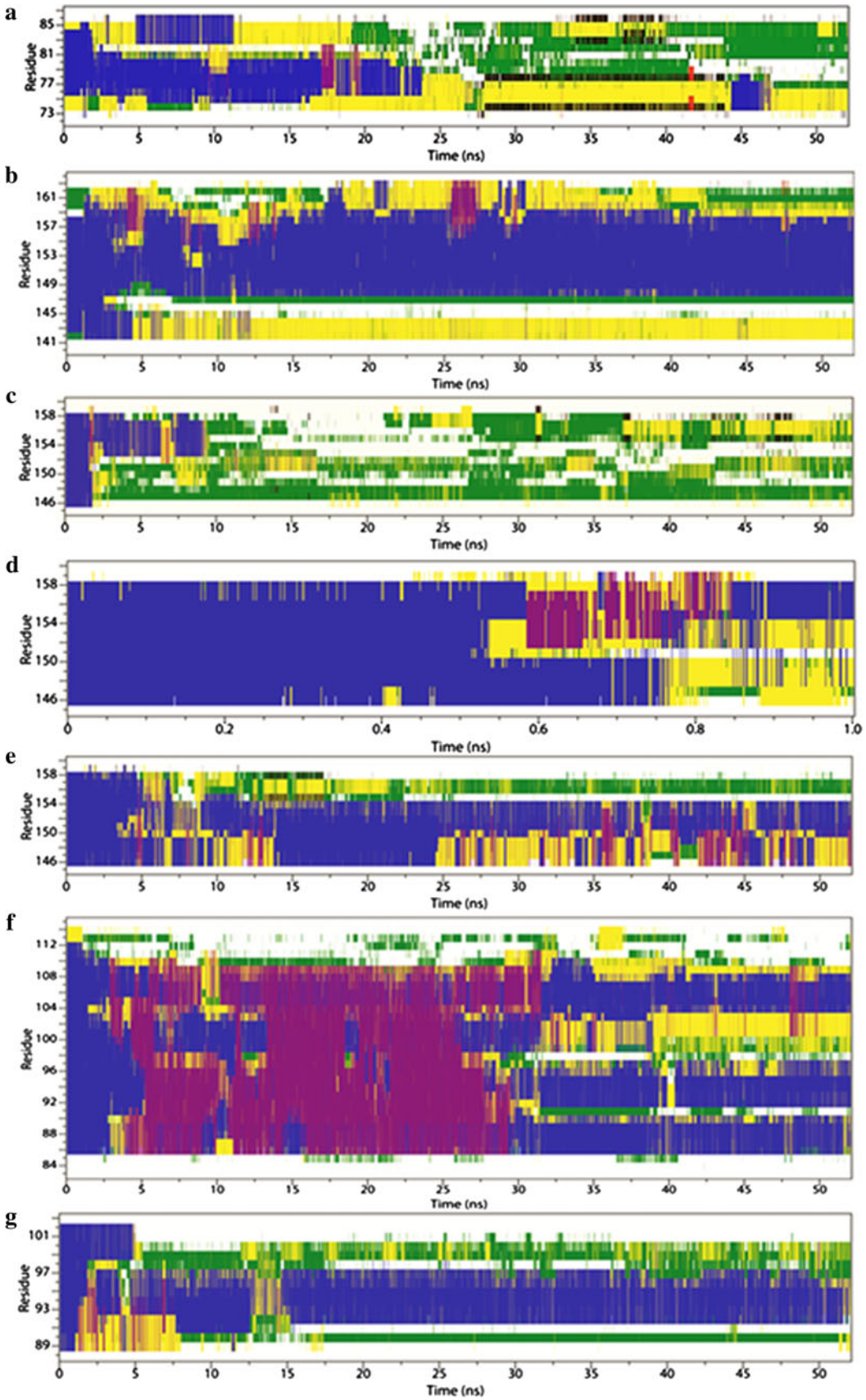
a
Residue
85
81
77
73
0 5 10 15 20 25 30 35 40 45 50
Time (ns)
b
Residue
161
157
153
149
145
141
0 5 10 15 20 25 30 35 40 45 50
Time (ns)
c
Residue
158
154
150
146
0 5 10 15 20 25 30 35 40 45 50
Time (ns)
d
Residue
158
154
150
146
0 0.2 0.4 0.6 0.8 1.0
Time (ns)
e
Residue
158
154
150
146
0 5 10 15 20 25 30 35 40 45 50
Time (ns)
f
Residue
112
108
104
100
96
92
88
84
0 5 10 15 20 25 30 35 40 45 50
Time (ns)
g
Residue
101
97
93
89
0 5 10 15 20 25 30 35 40 45 50
Time (ns)

remained helical. On the other hand, the secondary structure of the 16-mer mutant Bad peptide (Fig. 1e) shows that the helical character is maintained in the middle region of the peptide from residues 150–155 throughout the simulation. This is in sharp contrast to what was observed in the 16-mer wild type peptide where unwinding event was initiated around this region.

In the case of the 33-mer Bim (Fig. 1f) which is helical from residues 86–112 in the starting structure, we observe that the longer helical segment of the peptide collapses to form three short helical fragments by the end of the simulation period. One of the distinctive features of the plot is the substantial π-helix conformation adopted by the peptide during the simulation. The π-helix was previously reported as the least observed of the three helices (α-helix, 3_{10}-helix and π-helix) in the experimentally determined three dimensional structures and this was attributed to its instability due to multiple factors [43]. The occurrence of the π-helix during our molecular dynamics simulation could therefore be an artifact of the force field parameters. This was shown to be true in the simulation of the apoliprotein A-I derived peptide [44]. The peptide whose simulation was started from the α-helical state adopted a π-helix conformation using all atom CHARMM22 [45] force field whereas upon using of an improved CHARMM22/CMAP [46] force filed parameters, the π-helix was completely eliminated. However a recent study has also shown that π-helix which was believed to be geometrically and energetically unfavorable has been found to be relatively more prevalent than previously thought in experimental protein structures [43]. Similarly, in a simulation study of chain B of insulin, five different force fields were compared [47] and π-helix formation was observed when CHARMM27 force field [45] was used. Interestingly, the experimentally observed dynamic behavior of the peptide was best reproduced by CHARMM27 and GROMOS96 43a1 force fields. With our current simulation study on the 33-mer Bim peptide, one could argue that the occurrence of the π-helix could be due to the artifact of the GROMOS96 43a1 force field [35, 36] used in this simulation. Alternatively, this peptide's ability to adopt this distinct secondary structure cannot be completely ruled out. However, the peptide's π-helix conformation is stable only up to 30 ns following which it adopts a conformation consisting of three short α-helices which remained stable for the rest of the simulation. Hence, it is possible that π-helix may represent the intermediate helical secondary structure and formation of π-helical structure could indicate a transition between a long α-helical segment and several small helical segments of the 33-mer Bim peptide. The 16-mer Bim peptide (Fig. 1g) is almost completely helical in the starting structure but remains in the similar conformation for only a short period of the simulation. It begins to loose its helical character from the terminal regions but maintains a relatively stable helical segment in the middle of the peptide which is observed till the end of the simulation. It should be noted that the formation of π-helix is not observed in 16-mer Bim peptide.

Clustering of hydrophobic residues

Bak, Bad and Bim BH3 peptides are amphipathic in nature (Online Resource 1). The hydrophobic side of the peptides docks into the hydrophobic groove of Bcl-X_L protein [11, 22, 24]. In our simulations of isolated BH3 peptides, these residues are completely exposed to the solvent and hence the behavior of these hydrophobic residues during the simulations would be of immense interest to find out whether they contribute to the stability of the helix or result in helix unwinding. When they are part of a polypeptide chain, the hydrophobic residues tend to bury themselves in the interior of the protein. In the case of small peptides when exposed to aqueous medium, these residues are likely to cluster among themselves to minimize contact with water molecules. We have investigated this phenomenon by calculating the distance d_H as given in Eq. (1) described in the "Methods" section. For the purpose of residue classification, we used the hydrophobicity scale proposed by Jesior [48] which is based on 511 protein structures. According to this scale, the residues A, V, I, L, M, C, G, F, W and Y are classified as hydrophobic and the rest are hydrophilic.

Nine hydrophobic residues were identified in the 16-mer Bak peptide (G72, V74, G75, L78, A79, I80, I81, G82 and I85) and they are buried in the hydrophobic groove of the protein in the complex structure and many of them participate in peptide-protein interactions [11]. This includes the four conserved hydrophobic residues characteristic of a BH3 domain present in most of the Bcl-2 family proteins. Analysis of d_H trajectory shows that the parameter d_H is fairly stable up to 23 ns after the initial drop (Fig. 2a). A comparison with the Bak peptide's DSSP plot also reveals that Bak helix was stable till that time (Fig. 1a). We then observe a sudden fluctuation in the profile which coincides with the complete unwinding of the helix. Consequently the value of d_H also decreases suggesting that the hydrophobic residues show a clustering tendency. After about 40 ns, d_H increases again indicating that the peptide, after unwinding, is sampling different conformations in an attempt to find the best conformation that will maximally bury the hydrophobic residues. In the absence of other compensating interactions, the collapse of hydrophobic residues results in a complete loss of helical character for the 16-mer Bak peptide.

Eleven hydrophobic residues in 25-mer Bad (L141, W142, A143, A144, Y147, G148, L151, M154, F158,

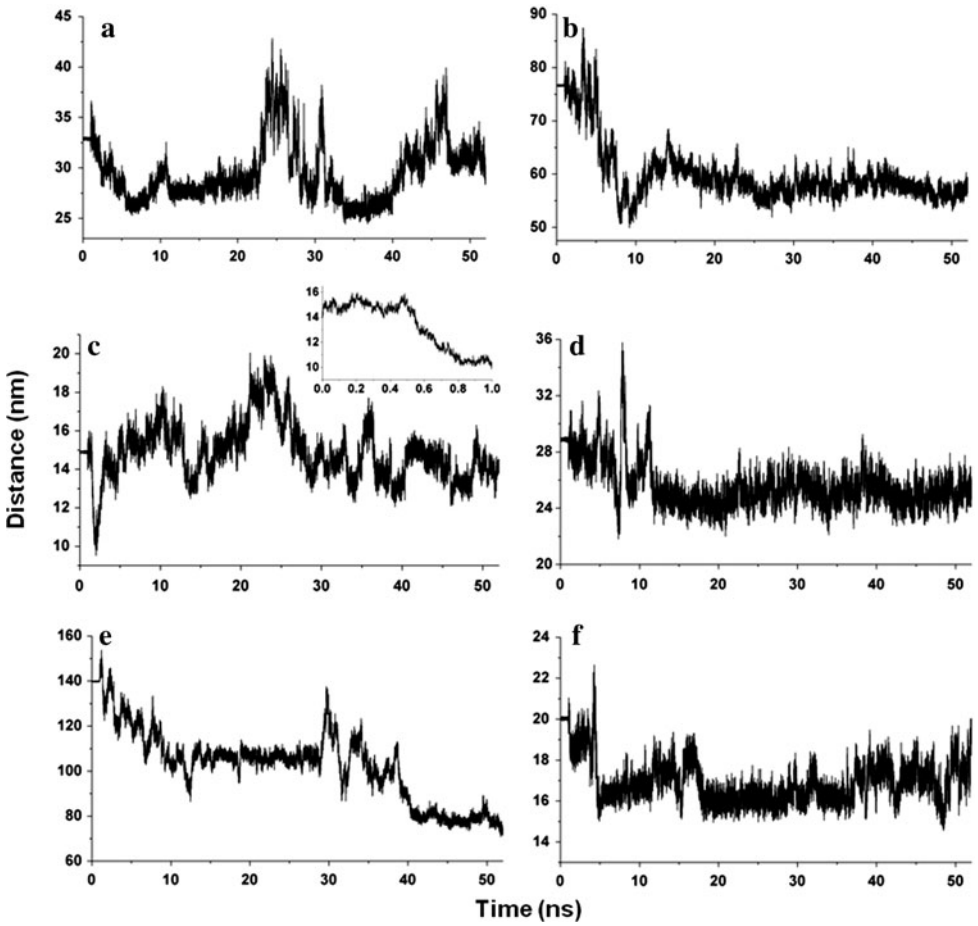

Fig. 2 Molecular dynamics trajectories of d_H as a function of simulation time: **a** 16-mer Bak, **b** 25-mer Bad, **c** 16-mer Bad wt, **d** 16-mer Bad mutant, **e** 33-mer Bim and **f** 16-mer Bim. For 16-mer Bad wt, the same analysis is shown for the last 1 ns of equilibration in the *inset* of **c**. For all other peptides, the MD trajectories are displayed for the entire 52 ns simulation which includes 2 ns equilibration run

V159 and F162) are identified and most are involved in interactions with the Bcl-X_L protein in the complex structure [22]. All eleven residues were considered to calculate the d_H trajectory for the 25-mer Bad peptide (Fig. 2b). It is clear that there is a sudden drop in d_H within the first 10 ns which nicely coincides with the unwinding of N- and C-terminal regions of the peptide during the same period (Fig. 1b). However, both the d_H and a large part of helical structure remained stable for the rest of the simulation. However, in the case of 16-mer wild-type Bad peptide, the helix unfolded early on in the simulation and a total unwinding was observed after 10 ns (Fig. 1c). In the 16-mer Bad wt case, the parameter d_H was calculated only for six residues (Y147, G148, L151, M154, F158 and V159) since the other five residues were missing due to truncation (Fig. 2c). The burial of the exposed hydrophobic residues occurred at the equilibration stage itself. This can be seen in the drastic decrease of d_H around 500 ps of 1 ns restraint-free equilibration (Fig. 2c, inset). The peptide's helical conformation also started to destabilize around this period (Fig. 1d). In the case of 16-mer Bad mutant, six residues were mutated to increase the helix propensity and the simulation of this peptide did result in a stable helical structure (Fig. 1e). To calculate d_H, eight hydrophobic residues were considered which is two more than that considered for the wild-type 16-mer. This is due to the fact that two of the hydrophilic residues in the wild-type peptide were mutated to hydrophobic residues (R153 → M and S155 → A). Analysis of d_H trajectory for the mutant Bad peptide shows that after the initial fluctuation which lasted up to 10 ns, a stable profile was observed for rest of the production run (Fig. 2d). The fluctuation in d_H also coincides with the decrease in the helical character of the peptide (Fig. 1e). This analysis further reiterates that the process of clustering of exposed hydrophobic residues disturbs the helical conformation of the peptide and has a role in the loss of the helical character of the Bad peptides.

The 33-Bim peptide is the longest BH3 peptide simulated in this study. For the purpose of analyzing d_H, thirteen hydrophobic residues (L84, I88, I90, A91, L94, I97, G98, F101, Y105, V109, F110, A111, and Y114) were considered. There was a drastic decrease in the value of d_H initially and then it stayed stable till about 30 ns of the simulation (Fig. 2e). Around this time, there is a sudden transient increase in d_H followed by a rapid decrease suggesting further burial of the hydrophobic residues. This behavior around 30 ns which can be described equivalent to a hydrophobic collapse nicely correlates with the time

period at which the helical structure of the peptide is also destabilized (Fig. 1f). This results in three smaller helical fragments of 33-mer Bim peptide. The stabilization of these smaller helical fragments (see below) and further burial of hydrophobic residues from helical and non-helical regions explains further decrease of d_H after 40 ns. In case of the 16-mer Bim peptide, the hydrophobic residues (I88, I90, A91, L94, I97, G98 and F101) tend to cluster themselves very early in the simulation as seen by the decrease in d_H (Fig. 2f). The destabilization of helical structure in the terminal regions could possibly be linked to the burial of the hydrophobic residues from these regions (Fig. 1g). As observed in other BH3 peptides, hydrophobic residues tend to cluster together to minimize their exposure to water molecules and this factor is a major driving force for loss in helical character of all the BH3 peptides including Bim.

Stability of helical segments in BH3 peptides

Analysis of BH3 peptide helices as a function of simulation time clearly revealed that not all BH3 helices are equally stable when present in an aqueous medium. Even when the peptide length is same, 16-mer Bak and 16-mer Bad wt peptides adopted a completely random conformation by the end of the simulation period. However, the 16-mer Bad mutant and the wild-type 16-mer Bim peptides did exhibit a stable helical character at the end of 50 ns production run. Similarly, the longer 25-mer Bad and 33-mer Bim peptides also possess helical segments that remained stable in aqueous medium. The reasons behind the stable helical segments of these BH3 peptides could be clearly understood at molecular level if we carefully analyze the intramolecular interactions within each peptide and the interactions between the peptide and the water molecules.

16-mer Bak, Bad and Bim BH3 peptides

The starting structure of 16-mer Bad wt peptide along with the side-chains of four conserved hydrophobic residues is shown in Fig. 3a. During the simulation, the exposed hydrophobic residues in Bad and the hydrophobic residues in equivalent positions (Table 1) in other BH3 peptides tend to bury themselves and this is observed in all 16-mer BH3 peptides (Fig. 3b, c, e, f). The 16-mer Bad mutant and 16-mer Bim peptides have stabilizing interactions in the hydrophilic side of the helix (Fig. 3d, g). Such interactions include hydrogen bond formation between side-chains of hydrophilic residues and interactions involving capping residues and these are explained in the following sections. Absence of such favorable interactions in the hydrophilic side and collapse of hydrophobic residues result in complete loss of helical structure in 16-mer Bak and 16-mer Bad wt peptides.

16-mer wild-type Bad vs 25-mer wild-type Bad

The DSSP plot of 25-mer Bad peptide clearly revealed that the N-terminal region is no longer helical at the end of 50 ns simulation (Fig. 1b). The first two turns of the helix in the N-terminal end clearly unwound and folded back on the rest of the helical segment (Fig. 4a). This actually helped to bury clusters of hydrophobic residues such as L141, W142, A143, A144 and Y147. Center of mass distances between each of these residues and the other hydrophobic residues in the peptide were monitored. Among all pairs of hydrophobic residues, the decrease in the distances for the hydrophobic residue pairs (W142, M154) and (W142, F158) are the most noticeable. In the starting structure, the distances between (W142, M154) and (W142, F158) were close to 13 and 21 Å respectively. As the simulation progressed, W142 positioned itself between M154 and F158 residues which are exactly one above the other in the helical conformation. Such an arrangement helped W142 to bury itself from the aqueous medium and made stable contact with both M154 and F158 residues (Table 2). The average distances calculated during the last 5 ns of production run for both the residue pairs are 3.7 and 3.8 Å respectively. Such strong and stable interactions between the residues W142, M154 and F158 could be one of the major factors for the helical stability of the peptide. This even offsets the otherwise repulsive arrangement of the basic residues in the structure (R149, R152 and R153) in the hydrophilic side. The absence of extended N-terminus in 16-mer Bad wt implies that the residues M154 and F158 are vulnerable to exposure to the solvent and in the process of burying these hydrophobic residues, the helical structure in the 16-mer Bad wt is completely lost. The 25-mer Bad peptide is reported to have almost 800-fold higher affinity for Bcl-X_L than the 16-mer peptide which is attributed to its higher helical content [22]. The authors also suggested through mutagenesis study that the additional N and C-terminal residues (Table 1) had little role in its increased affinity through direct interaction with the protein but were rather involved in increasing the helical nature of the peptide. Our simulation study has lent support to such a suggestion and provided explanation at molecular level that the tryptopthan residue present at the N-terminal region could be responsible in the overall stability of the helical character of the 25-mer Bad peptide in solution.

16-mer Bad wt vs 16-mer Bad mutant

It has been shown that the helical content of 16-mer Bad peptide has increased from 7 to 46% when certain residues were mutated (Table 1) and correspondingly, the binding affinity also has increased from $K_d = 50{,}000$ nM to

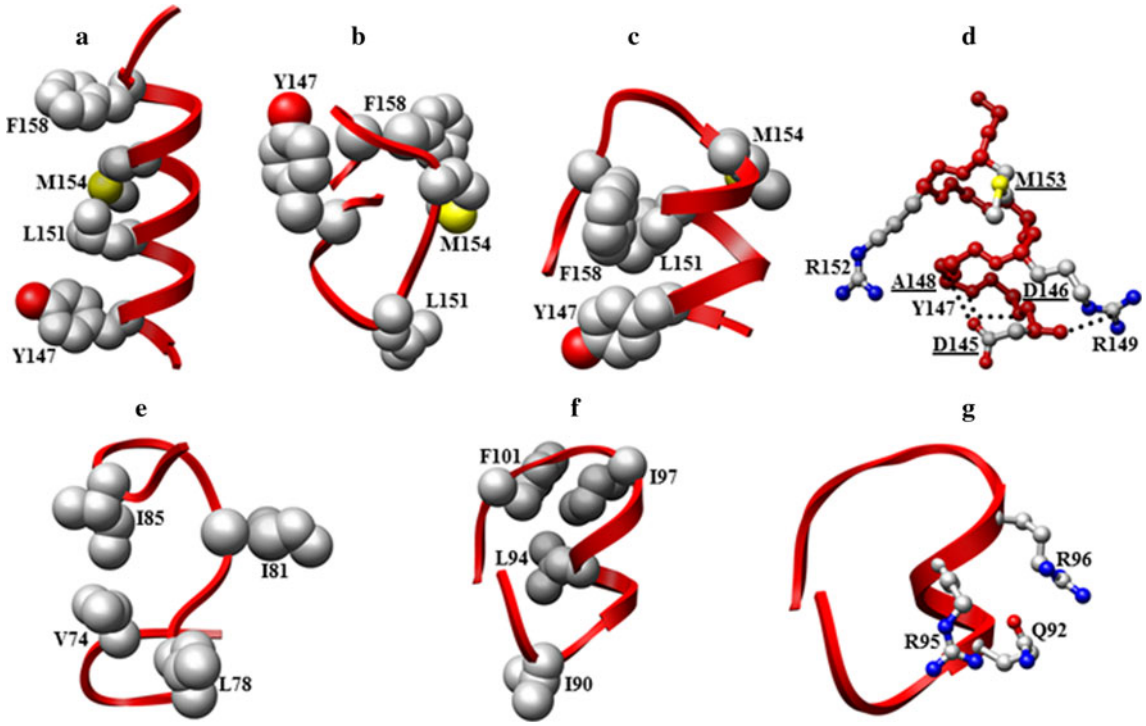

Fig. 3 Structures of different 16-mer BH3 peptides are shown. **a** The initial structure of 16-mer Bad wt. Structures saved at the end of 50 ns production run for **b** 16-mer Bad wt, **c**, **d** 16-mer Bad mutant, **e** 16-mer Bak and **f**, **g** 16-mer Bim BH3 peptides. A ball-and-stick representation is used in **d** and in the other figures, the backbone is shown as ribbon. The four conserved hydrophobic residues are displayed in space-filling representation and are labeled. Residues participating in stabilizing interactions in the hydrophilic side of the peptide are labeled and shown for the **d** 16-mer Bad mutant and **g** 16-mer Bim peptides. The mutated residues in 16-mer Bad mutant peptide in **d** are *underlined*. All molecular plots were created using the UCSF chimera package [56]

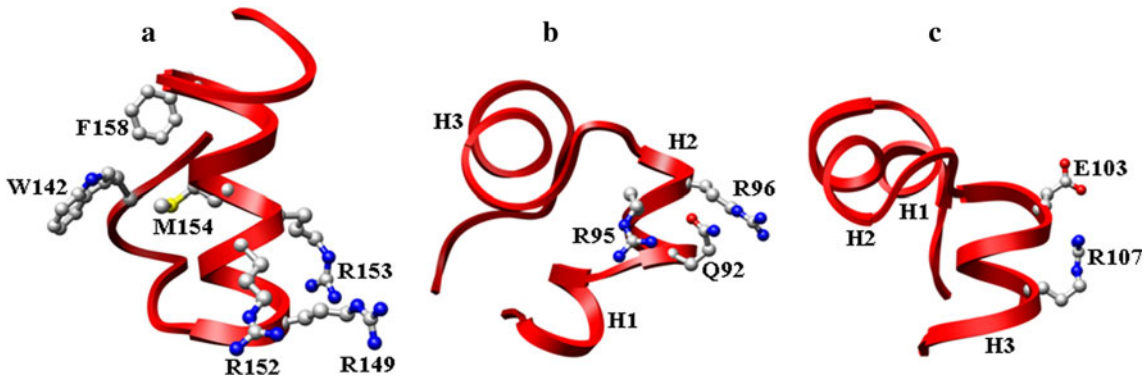

Fig. 4 Structures of longer BH3 peptides **a** 25-mer Bad and **b**, **c** 33-mer Bim saved at the end of 50 ns production run. The backbone of the peptides is shown in ribbon representation. Residues participating in interactions are shown in ball-and-stick representation. The three short helical segments in the 33-mer Bim peptide are labeled as H1, H2 and H3. Two different orientations of the Bim peptide are shown to highlight the stabilizing interactions that occur in **b** H2 and **c** H3

K_d = 203 nM [22]. Here, only the solvent exposed residues were mutated to helix-promoting residues. MD simulation of the 16-mer Bad mutant peptide clearly revealed a stable helix supporting the experimental observations (Fig. 3c). This is in contrast to the wild-type 16-mer Bad peptide which completely lost its helical character and adopted a random conformation at the end of the production run. It must be noted that the conserved hydrophobic residues Y147, L151, M154 and F158 which are involved in contact with the protein were unchanged in the mutant peptide (Fig. 3c). One would be curious to know how these exposed hydrophobic residues behave in the wild-type and mutated 16-mer Bad peptides. In the case of 16-mer Bad wt peptide, the N-terminal Y147 residue comes close to the two C-terminal hydrophobic residues at the end of 50 ns production run resulting in the total unwinding of the

Table 2 Center of mass distances (in Å) between pairs of hydrophobic residues in BH3 Bad peptides

Residue pairs[a]	16-mer Bad wt[b]	16-mer Bad mutant[b]	25-mer Bad[b]
W142–M154	N/A	N/A	12.8; 3.7 (0.3)
W142–F158	N/A	N/A	20.7; 3.8 (0.5)
Y147–L151	6.4; 13.1 (0.8)	6.4; 5.3 (0.5)	6.4; 6.7 (0.4)
Y147–M154	10.5; 9.9 (0.5)	10.5; 10.5 (0.8)	10.5; 11.0 (0.4)
Y147–F158	15.7; 9.8 (0.8)	15.7; 6.8 (0.7)	15.7; 15.5 (0.5)
L151–M154	4.9; 8.7 (1.1)	4.9; 5.6 (0.9)	4.9; 5.3 (0.2)
L151–F158	9.6; 11.8 (1.5)	9.6; 5.2 (0.6)	9.6; 9.9 (0.3)
M154–F158	7.5; 5.7 (1.2)	7.5; 8.7 (0.8)	7.5; 5.0 (0.3)

[a] The residues Y147, L151, M154 and F158 are the conserved hydrophobic residues and all possible pairs among these four residues are considered for this analysis to understand the behavior of solvent exposed hydrophobic residues

[b] The distance calculated for the starting structure and the average distance (standard deviation) calculated for the last 5 ns of the simulations are both reported and they are delineated by a semi-colon (;)

helical structure (Table 2) (Fig. 3b). However, the 16-mer Bad mutant peptide manages to maintain its helical conformation by bringing the C-terminal F158 residue close to Y147 and L151 (Table 2). In this process, only the last turn of the helix is destabilized (Fig. 3c). This is unlike the 16-mer Bad wt peptide. Although clustering of hydrophobic residues is a common phenomenon for both the 16-mer Bad peptides, molecular investigation revealed multiple factors to be responsible for the helical stability of the 16-mer Bad mutant peptide.

Multiple stabilizing interactions of different nature occur in the hydrophilic side of the mutant BH3 peptide. The mutation of R153 to Met residue resulted in a favorable contact with R149 residue which is located one turn below the helix. The interaction with M153 is mostly mediated through the acyl portion of R149 and as such the interaction could be described as hydrophobic in nature. In addition, the guanidium group of R149 forms a relatively stable contact with the backbone nitrogen atom from D145 which is again a mutated residue (Q145D). Since this interaction involves the mainchain atom of D145, it may exist irrespective of the amino acid at position 145. Both the interactions involving the residue pairs (R149, M153) and (R149, D145) could contribute to the stability of the helical segment (Fig. 3d). The mutation Q145D appears to be critical, since as a N-cap residue, Asp is known to stabilize the helix [49]. The side chain carbonyl oxygen atoms of N-terminal Asp residue, when it occurs as the first helical residue i, can form hydrogen bonds with the backbone amide nitrogen atoms of residues $i + 1$, $i + 2$ or $i + 3$ which are not involved in intra-helical hydrogen bonds. D145 is the first residue in the 16-mer Bad mutant peptide and the minimum distance between the carbonyl oxygens of D145 and the backbone nitrogen atoms of D146, Y147 and A148 is respectively 4.5, 7.5 and 7.5 Å in the starting structure. D146 and A148 are mutated residues from the wild type R146 and G148 residues. During the simulation, the average minimum distance between the atoms decreases to 3–3.5 Å. This capping role performed by D145 could be a major factor that might have prevented the unwinding of the helix in the N-terminus.

16-mer Bim and 33-mer Bim

Both 16-mer and 33-mer wild-type Bim peptides exhibit stable helical segments during the course of 50 ns simulation. A closer examination of both peptides reveals the factors that are responsible for stable helical segments. A common feature observed between the helical segments of both the peptides is the clustering of hydrophobic residues on one face of the helix and stable hydrogen bond interactions on the other face which is exposed to the solvent when the peptide is present in the complex structure. Hydrogen bonds form between the side-chain of Q92 and the guanidium group present in the two Arg side-chains R95 and R96.

In the structure of the 33-mer Bim peptide at the end of the simulation (Fig. 4b, c), the peptide is broken into three short helices which are designated as H1, H2 and H3. The possible reasons why these regions have stable helical character were investigated further. As in other peptides, the long 33-mer peptide collapses early in the simulation to bury its hydrophobic residues. The stability of N-terminal helical segment H1 (residues 86–90) could be attributed to the stable interactions between such hydrophobic residues. The helical segment H2 (residues 92–97) is the same as the stable helical region observed for the 16-mer Bim peptide and the factors stabilizing the helical character have been discussed above. The segment H3 is stabilized by a stronger salt-bridge interaction formed between the side chain carboxyl oxygens of E103 and the guanidium group of R107 which occur one above the other in the helical conformation (Fig. 4c). Thus it appears that the hydrophobic interactions on one face of the helices coupled with hydrogen bond and salt-bridge interactions on the other face are reasons for the stability of the helical segments in the simulated 16-mer and 33-mer Bim peptides.

Discussion

One of the factors suggested for the difference in the binding affinity of BH3 peptides for the anti-apoptotic Bcl-X_L protein is their inherent helical character in solution [22]. Although CD studies gave an indication of which BH3 peptides exhibit more helical character, it was not

clear what factors are responsible for a stable helical structure for a given BH3 peptide. To answer this question, we have performed comparative molecular dynamics simulations of six BH3 peptides derived from three pro-apoptotic proteins, namely, Bak, Bad and Bim.

The peptide simulations were carried out as an unfolding study where the starting conformations of all the six peptides are mostly helical as observed in the Bcl-X_L complex structures. In general, an isolated α-helix is energetically not stable in aqueous solution since the water molecules compete to form hydrogen bonds with the backbone functional groups which participate in intra-helical hydrogen bonds. However, multiple factors such as sequence composition, capping motifs present at the terminal ends, side-chain interactions and helix length can influence the helical stability [49–53]. The BH3 peptides are predominantly amphipathic in nature (Online Resource 1). An isolated helical peptide of such nature will expose the hydrophobic side to water molecules in an aqueous medium and such a situation will be energetically unfavorable. All the BH3 peptide simulations clearly show that the hydrophobic residues tend to come close together to minimize the exposure to water medium. With the exception of Bad wild-type 16-mer, analysis of the potential energies of the peptides indicates that the structure at the end of 50 ns production run is energetically more favorable than the starting structure (Table 3). The energetically favorable conformation of the peptides corresponds to the relative loss in their helical character as compared to the starting structure. A common cause for this loss in helicity of all the peptides is the phenomena of hydrophobic collapse whereby hydrophobic residues are brought together and shielded from the solvent as much as possible. In this process, they bring about a change in the conformation of the peptides. The degree in the loss of helical character varied among different BH3 peptides. Among the four 16-mer peptides studied, two of them (16-mer Bak and 16-mer Bad) completely lost their helical character and adopt a random conformation. The 16-mer Bad mutant and the 16-mer Bim peptides maintain a portion of the peptide in helical conformation in solution. Among the longer peptide, 25-mer Bad maintains a relatively higher helical character and 33-mer Bim peptide adopts a compact structural fold with presence of multiple short helical segments in the solution. Apart from the clustering of hydrophobic residues, two types of additional interactions occur in the hydrophilic side of the peptide that can be related to stable helical segments. In the first type, if the residues that are solvent exposed in the complex structures and are separated by three to four residues, they participate in stabilizing hydrogen bond or salt-bridge interactions. In the second type, the capping residues participate in interactions that does not allow opening up the helical segment. This is especially true in the case of 16-mer Bad mutant peptide. Thus, this simulation study has clearly shown that the BH3 peptides have differences in maintaining their helical stability and these differences are mainly due to the different types of stabilizing interactions in the hydrophilic face of the peptide and in the N-terminal capping region.

Relationship between the helical content and the binding affinity

The sequences of the three BH3 Bad peptides that are simulated have been experimentally studied by Petros et al. for their helix-forming capability and affinity for Bcl-X_L [22]. Our analysis show that 16-mer Bad peptide has the least stable helical character in the solution and exists mostly in the random conformation (Fig. 1c). The 25-mer Bad (Fig. 1b) and 16-mer mutant Bad (Fig. 1e) on the other hand is predicted to have a more stable secondary helical structure. This data is in qualitative agreement to the experiment [22] which shows that 16-mer Bad peptide has only 7% helix in 30% TFE solution as compared to 25-mer and 16-mer Bad mutant peptides which have respectively 44% and 46% helical content. The 16-mer Bad was subsequently shown to have negligible affinity for Bcl-X_L (K_d of 50,000 nM) while 25-mer and the mutant 16-mer Bad have a remarkably higher affinity (K_d of 0.6 nM and 203 nM respectively). The comparative secondary structure evolution for the 16-mer Bak (Fig. 1a), 25-mer Bad (Fig. 1b) and 33-mer Bim (Fig. 1f) shows that the Bak peptide has the least stable helical character as compared to Bad and Bim. According to binding affinity studies, Bak has lower affinity for Bcl-X_L with K_d value of 480 nM as compared to Bad (K_d of 0.6 nM) [22] and Bim (K_d of 9.2 nM) [54] highlighting the correlation between helical stability in solution and affinity. This is also substantiated by our observation in the complex state simulations where the Bak peptide showed the least stable helical character [6]. Thus this simulation study is in excellent qualitative agreement with the experimental observations and strengthens the idea that the helix forming capability of the BH3 peptides has a significant role in defining the affinity of the peptides for Bcl-X_L. In addition to helix content, other factors such as amino acid composition, peptide length and the interacting residues from the anti-apoptotic partner [6] must also be taken into account and they are likely to influence the binding affinity of BH3 peptides.

The simulated structures of the BH3 peptides were analyzed to investigate the residues which remain in the helical region for the major duration of the simulation period. The backbone dihedral value ($-140° \leq \varphi \leq -30°$ and $-90° \leq \psi \leq +45°$) [55] of the individual residues was used to classify a residue being in helical or in non-helical region. A helical segment was defined with at least

Table 3 Average (standard deviation) potential energies (in KJ/mol) calculated for the first and last 10 ns of production runs

BH3 Peptides	Self-energy (KJ/mol)		Peptide-Solvent (KJ/mol)	
	First 10 ns	Last 10 ns	First 10 ns	Last 10 ns
16-mer Bak	−573 (134.6)	−749.6 (131.6)	−2,737.8 (268.1)	−2,441.4 (246.2)
25-mer Bad	−957.7 (246.5)	−1,407.4 (164.6)	−5,995.5 (484.0)	−5,221.4 (361.4)
16-mer Bad wt	−830.6 (227.5)	−728.4 (149.5)	−4,155.3 (458.8)	−4,265.9 (345.5)
16-mer Bad mutant	−461.1 (165.6)	−567.3 (153.0)	−4,572.4 (321.4)	−4,320.9 (345.5)
33-mer Bim	−1,816.7 (287.8)	−2,269.2 (268.4)	−7,319.1 (428.0)	−6,535.6 (482.5)
16-mer Bim	−606.2 (230)	−656.9 (193.6)	−3,980.9 (465.5)	−4,001.2 (378.2)

four consecutive α-helical residues in the helical conformation for at least 80% of the simulation time. The helical segments of the individual peptides identified using the above mentioned criteria are superimposed and are shown in Fig. 5. The stable helical segment that is common to all the BH3 peptides is comprised of a short five residue region with the conserved Leu located in the middle. This Leu residue is the most critical residue for the interaction of the pro-apoptotic BH3 peptides to anti-apoptotic Bcl-2 proteins as has been shown through structural and mutational studies [11, 19, 22]. The formation of short helical segments around the conserved Leu could be a crucial step that could facilitate the initial docking process of the peptide with the protein as opposed to any random conformation. This initial contact is likely to be a critical step in the Bcl-2 protein—BH3 peptide interaction and the affinity could be directly related to the propensity of this region to form a helical segment. Upon approaching the hydrophobic groove, the shorter helix may be extended due to the influence of environment. Thus this smaller helical segment around the conserved Leu could serve as a nucleation signal for an eventual longer helix upon binding to Bcl-X_L.

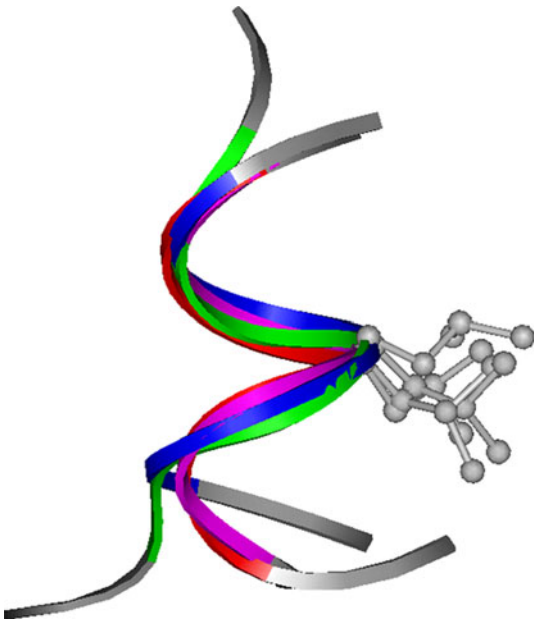

Fig. 5 Superposition of the stable helical segments observed at the end of 50 ns simulations for 16-mer Bim, 16-mer Bad mutant, 25-mer Bad and 33-mer Bim peptides (shown in *different colors*). Only the common helical region observed to be stable in all the four peptides are superposed. This region encompasses the conserved Leu residue which is shown in ball-and-stick representation

Conclusions

Inhibitors of anti-apoptotic Bcl-2 proteins have a great potential to be considered as anti-cancer drugs. Understanding the specificity of BH3 peptides from different pro-apoptotic proteins will help in developing peptide-based inhibitors that can target a particular anti-apoptotic Bcl-2 protein. Both the length of a peptide and its amino acid sequence are important for a BH3 peptide's higher binding affinity to a Bcl-2 anti-apoptotic protein. In this paper, we have also investigated a third factor, namely, its helical content in aqueous medium. Although CD spectroscopy studies indicated a relationship between a BH3 peptide's overall helical content and its binding affinity to Bcl-X_L protein, it is not clear how and why a certain BH3 peptide should adopt a stable helical segment. Molecular dynamics simulations of six BH3 peptides revealed that the hydrophobic residues in these amphipathic peptides tend to cluster themselves to avoid exposure to the solvent molecules. While this process is common to all the BH3 peptides, only certain peptides retain some helical character and the same is completely lost for other BH3 peptides. Favorable interactions between residues in the hydrophilic side that are separated by three/four residues and capping interactions are the two major factors that are responsible for giving rise to stable helical fragments. In the BH3 peptides simulated in this study, the stable helical fragments encompass the conserved Leu residue and we speculate that this is especially important for the BH3 peptides to bind to the hydrophobic groove of the anti-apoptotic protein. Before binding, the environment provided by the hydrophobic groove could induce and help extending the helical region on both N- and

C-terminal sides beyond the small helical fragment around the conserved Leu residue. The observations reported in this study could aid in designing peptide-based ligands that can adopt a more stable helical structure and hence could have an increased binding affinity for a specific Bcl-2 anti-apoptotic protein.

Acknowledgments The Joy Gill Chair Professorship to RS is gratefully acknowledged. We thank all members of our lab for useful discussions.

References

1. Jorgensen WL (2004) The many roles of computation in drug discovery. Science 303:1813–1818
2. Patgiri A, Jochim AL, Arora PS (2008) A hydrogen bond surrogate approach for stabilization of short peptide sequences in alpha-helical conformation. Acc Chem Res 41:1289–1300
3. Bellmann-Sickert K, Beck-Sickinger AG (2010) Peptide drugs to target G protein-coupled receptors. Trends Pharmacol Sci 31:434–441
4. Sankararamakrishnan R (2006) Recognition of GPCRs by peptide ligands and membrane compartments theory: structural studies of endogenous peptide hormones in membrane environment. Biosci Rep 26:131–158
5. Creamer TP, Rose GD (1994) Alpha-helix-forming propensities in peptides and proteins. Proteins Struct Funct Bioinform 19:85–97
6. Lama D, Sankararamakrishnan R (2008) Anti-apoptotic Bcl-X_L protein in complex with BH3 peptides of pro-apoptotic Bak, Bad, and Bim proteins: comparative molecular dynamics simulations. Proteins Struct Funct Bioinform 73:492–514
7. Danial NN (2007) Bcl-2 family proteins: critical checkpoints of apoptotic cell death. Clin Cancer Res 13:7254–7263
8. Skommer J, Wlodkowic D, Deptala A (2007) Larger than life: mitochondria and the Bcl-2 family. Leuk Res 31:277–286
9. Adams JM, Cory S (2001) Life-or-death decisions by the Bcl-2 protein family. Trends Biochem Sci 26:61–66
10. Youle RJ, Strasser A (2008) The Bcl-2 protein family: opposing activities that mediate cell death. Nat Rev Mol Cell Biol 9:47–59
11. Sattler M, Liang H, Nettesheim D, Meadows RP, Harlan JE, Eberstadt M, Yoon HS, Shuker SB, Chang BS, Minn AJ, Thompson CB, Fesik SW (1997) Structure of Bcl-X_L-Bak peptide complex: recognition between regulators of apoptosis. Science 275:983–986
12. Chittenden T, Flemington C, Houghton AB, Ebb RG, Gallo GJ, Elangovan B, Chinnadurai G, Lutz RJ (1995) A conserved domain in Bak, distinct from BH1 and BH2, mediates cell death and protein binding functions. EMBO J 14:5589–5596
13. Zha J, Harada H, Osipov K, Jockel J, Waksman G, Korsmeyer SJ (1997) BH3 domain of BAD is required for heterodimerization with Bcl-X_L and pro-apoptotic activity. J Biol Chem 272: 24101–24104
14. Kelekar A, Thompson CB (1998) Bcl-2-family proteins: the role of the BH3 domain in apoptosis. Trends Cell Biol 8:324–330
15. Holinger EP, Chittenden T, Lutz RJ (1999) Bak BH3 peptides antagonize Bcl-X_L function and induce apoptosis through cytochrome c-independent activation of caspases. J Biol Chem 274:13298–13304
16. Chittenden T (2002) BH3 domains: intracellular death-ligands critical for initiating apoptosis. Cancer Cell 2:165–166
17. Lessene G, Czabotar PE, Colman PM (2008) Bcl-2 family antagonists for cancer therapy. Nat Rev Drug Discov 7:989–1000
18. Letai A, Bassik MC, Walensky LD, Sorcinelli MD, Weiler S, Korsmeyer SJ (2002) Distinct BH3 domains either sensitize or activate mitochondrial apoptosis, serving as prototype cancer therapeutics. Cancer Cell 2:183–192
19. Chen L, Willis SN, Wei A, Smith BJ, Fletcher JI, Hinds MG, Colman PM, Day CL, Adams JM, Huang DC (2005) Differential targeting of prosurvival Bcl-2 proteins by their BH3-only ligands allows complementary apoptotic function. Mol Cell 17:393–403
20. Vogler M, Dinsdale D, Dyer MJ, Cohen GM (2009) Bcl-2 inhibitors: small molecules with a big impact on cancer therapy. Cell Death Differ 16:360–367
21. Kang MH, Reynolds CP (2009) Bcl-2 inhibitors: targeting mitochondrial apoptotic pathways in cancer therapy. Clin Cancer Res 15:1126–1132
22. Petros AM, Nettesheim DG, Wang Y, Olejniczak ET, Meadows RP, Mack J, Swift K, Matayoshi ED, Zhang H, Thompson CB, Fesik SW (2000) Rationale for Bcl-X_L/Bad peptide complex formation from structure, mutagenesis, and biophysical studies. Protein Sci 9:2528–2534
23. Shangary S, Oliver CL, Tillman TS, Cascio M, Johnson DE (2004) Sequence and helicity requirements for the proapoptotic activity of Bax BH3 peptides. Mol Cancer Ther 3:1343–1353
24. Liu X, Dai S, Zhu Y, Marrack P, Kappler JW (2003) The structure of a Bcl-X_L/Bim fragment complex: implications for Bim function. Immunity 19:341–352
25. Bierzynski A (2001) Methods of peptide conformation studies. Acta Biochim Pol 48:1091–1099
26. Wu X, Wang S (2001) Helix folding of an alanine-based peptide in explicit water. J Phys Chem B 105:2227–2235
27. Wang W-Z, Lin T, Sun Y-C (2007) Examination of the folding of a short alanine-based helical peptide with salt bridges using molecular dynamics simulation. J Phys Chem B 111:3508–3514
28. Villa A, Mark AE, Saracino GA, Cosentino U, Pitea D, Moro G, Salmona M (2006) Conformational polymorphism of the PrP106–126 peptide in different environments: a molecular dynamics study. J Phys Chem B 110:1423–1428
29. Nordling E, Kallberg Y, Johansson J, Persson B (2008) Molecular dynamics studies of alpha-helix stability in fibril-forming peptides. J Comput Aided Mol Des 22:53–58
30. Guo Z, Mohanty U, Noehre J, Sawyer TK, Sherman W, Krilov G (2010) Probing the α-helical structural stability of stapled p53 peptides: molecular dynamics simulations and analysis. Chem Biol Drug Des 75:348–359
31. Yang CY, Nikolovska-Coleska Z, Li P, Roller P, Wang SM (2004) Solution conformations of wild-type and mutated Bak BH3 peptides via dynamical conformational sampling and implication to their binding to antiapoptotic Bcl-2 proteins. J Phys Chem B 108:1467–1477
32. UniProt Consortium. The Universal Protein Resource (UniProt) (2009) Nucleic Acids Res 37:D169–D174
33. Lindahl E, Hess B, van der Spoel D (2001) Gromacs 3.0: a package for molecular simulation. J Mol Model 7:306–317
34. van der Spoel D, Lindahl E, Hess B, Groenhof G, Mark AE, Berendsen HJC (2005) GROMACS: fast, flexible, and free. J Comput Chem 26:1701–1718
35. Daura X, Mark AE, van Gunsteren WF (1998) Parametrization of aliphatic CHn united atoms of GROMOS96 force field. J Comput Chem 19:535–547
36. van Gunsteren WF, Billeter SR, Eising AA, Hunenberger PH, Kruger P, Mark AE, Scott WRP, Tironi IG (1996) Biomolecular simulation: The GROMOS96 manual and user guide. Vdf Hochschulverlag AG an der ETH Zurich, Switzerland, pp 1–1042
37. Berendsen HJC, Postma JPM, van Gunsteren WF,Hermans J (1981) In: Pullman B (ed) Interaction models for water in relation

to protein hydration. Intermolecular Forces. Reidel, Dordrecht, pp 331–342
38. Miyamoto S, Kollman PA (1992) SETTLE: an analytical version of the shake and rattle algorithm for rigid water models. J Comput Chem 13:952–962
39. Hess B, Bekker H, Berendsen HJC, Fraaije JGEM (1997) LINCS: a linear constraint solver for molecular simulations. J Comput Chem 18:1463–1472
40. Berendsen HJC, Postma JPM, van Gunsteren WF, Dinola A, Haak JR (1984) Molecular-dynamics with coupling to an external bath. J Chem Phys 81:3684–3690
41. Kabsch W, Sander C (1983) Dictionary of protein secondary structure: pattern recognition of hydrogen-bonded and geometrical features. Biopolymers 22:2577–2637
42. Wu X, Wang S (1998) Self-guided molecular dynamics simulation for efficient conformational search. J Phys Chem B 102:7238–7250
43. Fodje MN, Al-Karadaghi S (2002) Occurrence, conformational features and amino acid propensities for the pi-helix. Protein Eng 15:353–358
44. Stavrakoudis A (2008) Molecular dynamics simulations of an apoliprotein A-I derived peptide in explicit water. Chem Phys Lett 461:294–299
45. MacKerell AD Jr, Bashford D, Bellott M, Dunbrack RL Jr, Evanseck JD, Field MJ, Fischer S, Gao J, Guo H, Ha S, Joseph-McCarthy D, Kuchnir L, Kuczera K, Lau FTK, Mattos C, Michnick S, Ngo T, Nguyen DT, Prodhom B, Reiher WE III, Roux B, Schlenkrich M, Smith JC, Stote R, Straub J, Watanabe M, Wiorkiewicz-Kuczera J, Yin D, Karplus M (1998) All atom empirical potential for molecular modeling and dynamics studies of proteins. J Phys Chem B 102:3586–3616
46. MacKerell AD Jr, Feig M, Brooks CL III (2004) Improved treatment of the protein backbone in empirical force fields. J Am Chem Soc 126:698–699
47. Todorova N, Legge FS, Treutlein H, Yarovsky I (2008) Systematic comparison of empirical forcefields for molecular dynamic simulation of insulin. J Phys Chem B 112:11137–11146
48. Jesior J-C (2000) Hydrophilic framework in proteins? J Protein Chem 19:93–103
49. Serrano L, Fersht AR (1989) Capping and alpha-helix stability. Nature 342:296–299
50. Jain A, Purohit CS, Verma S, Sankararamakrishnan R (2007) Close contacts between carbonyl oxygen atoms and aromatic centers in protein structures: pi-pi or lone-pair-pi interactions? J Phys Chem B 111:8680–8683
51. Engel DE, DeGrado WF (2004) Amino acid propensities are position-dependent throughout the length of alpha-helices. J Mol Biol 337:1195–1205
52. Pal TK, Sankararamakrishnan R (2010) Quantum chemical investigations on intraresidue carbonyl-carbonyl contacts in aspartates of high-resolution protein structures. J Phys Chem B 114:1038–1049
53. Chakrabarti P, Pal D (2001) The interrelationships of side-chain and main-chain conformations in proteins. Prog Biophys Mol Biol 76:1–102
54. Kuwana T, Bouchier-Hayes L, Chipuk JE, Bonzon C, Sullivan BA, Green DR, Newmeyer DD (2005) BH3 domains of BH3-only proteins differentially regulate bax-mediated mitochondrial membrane permeabilization both directly and indirectly. Mol Cell 17:525–535
55. Eswar N, Ramakrishnan C (2000) Deterministic features of side-chain main-chain hydrogen bonds in globular protein structures. Protein Eng 13:227–238
56. Pettersen EF, Goddard TD, Huang CC, Couch GS, Greenblatt DM, Meng EC, Ferrin TE (2004) UCSF chimera—a visualization system for exploratory research and analysis. J Comput Chem 25:1605–1612